Journal of Power Sources 232 (2013) 1–6

Contents lists available at SciVerse ScienceDirect

Journal of Power Sources

journal homepage: www.elsevier.com/locate/jpowsour

Enhanced efficiency of bifacial and back-illuminated Ti foil based flexible dye-sensitized solar cells by decoration of mesoporous SiO_2 layer on TiO_2 anode

Kun-Mu Lee [a,b,*], Wei-Hao Chiu [a], Vembu Suryanarayanan [c], Chun-Guey Wu [a,d,*]

[a] Research Center for New Generation Photovolatics, National Central University, Taoyuan 32001, Taiwan
[b] Department of Chemical and Materials Engineering, National Central University, Taoyuan 32001, Taiwan
[c] Electroorganic Division, Central Electrochemical Research Institute, Karaikudi 630 006, Tamil Nadu, India
[d] Department of Chemistry, National Central University, Taoyuan 32001, Taiwan

HIGHLIGHTS

- Coating SiO_2 mesoporous layer on TiO_2 electrode improves the incident light into dye-sensitized solar cells.
- Coating SiO_2 layer on TiO_2 porous electrode shows an increase of J_{SC} by approximately 17.6%.
- Ti foil based flexible sub-module DSC (5 cm × 10 cm) shows high conversion efficiencies of 5.54% under 1 sun irradiation.

GRAPHICAL ABSTRACT

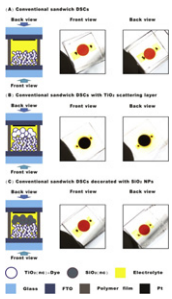

ARTICLE INFO

Article history:
Received 24 July 2012
Received in revised form
1 November 2012
Accepted 24 December 2012
Available online 11 January 2013

Keywords:
Back-illuminated
Dye-sensitized solar cells
Ti foil
Mesoporous film

ABSTRACT

The present study focuses on enhancing the efficiency of bifacial and back-illuminated dye-sensitized solar cells (DSCs) by incorporating SiO_2 mesoporous layer on TiO_2 electrode. The performance of DSCs is investigated by UV–visible spectroscopy, incident photon conversion efficiency (IPCE) and electrochemical impedance spectroscopy (EIS). It is observed that the current ratio of back- to front-DSC increases with the increase in the thickness of SiO_2 layer, which in turn influences the incident light to dyed-TiO_2 electrode, especially in the wavelength of 400–600 nm. The Ti foil based flexible small (0.28 cm^2) and sub-module (5 cm × 10 cm) DSCs having this modification show high conversion efficiencies of 6.76 and 5.54% respectively under 100 mW cm^{-2} (AM 1.5).

1. Introduction

Photovoltaic applications of dye-sensitized solar cells (DSCs) have been studied extensively in recent years due to their high conversion efficiency and low cost in fabrication [1,2]. A DSC generates photocurrent through ultra-fast injection of electrons from photo-excited dye molecules into the conduction band of a semiconductor such as TiO_2 or ZnO. This process is followed by dye regeneration and holes transportation to the counter electrode. In

* Corresponding authors. Research Center for New Generation Photovolatics, National Central University, Taoyuan 32001, Taiwan. Tel.: +886 3 4227151x25373; fax: +886 3 4252296.
E-mail addresses: kmlee@ncu.edu.tw, d93549007@ntu.edu.tw (K.-M. Lee).

0378-7753/$ – see front matter © 2013 Elsevier B.V. All rights reserved.
http://dx.doi.org/10.1016/j.jpowsour.2012.12.094

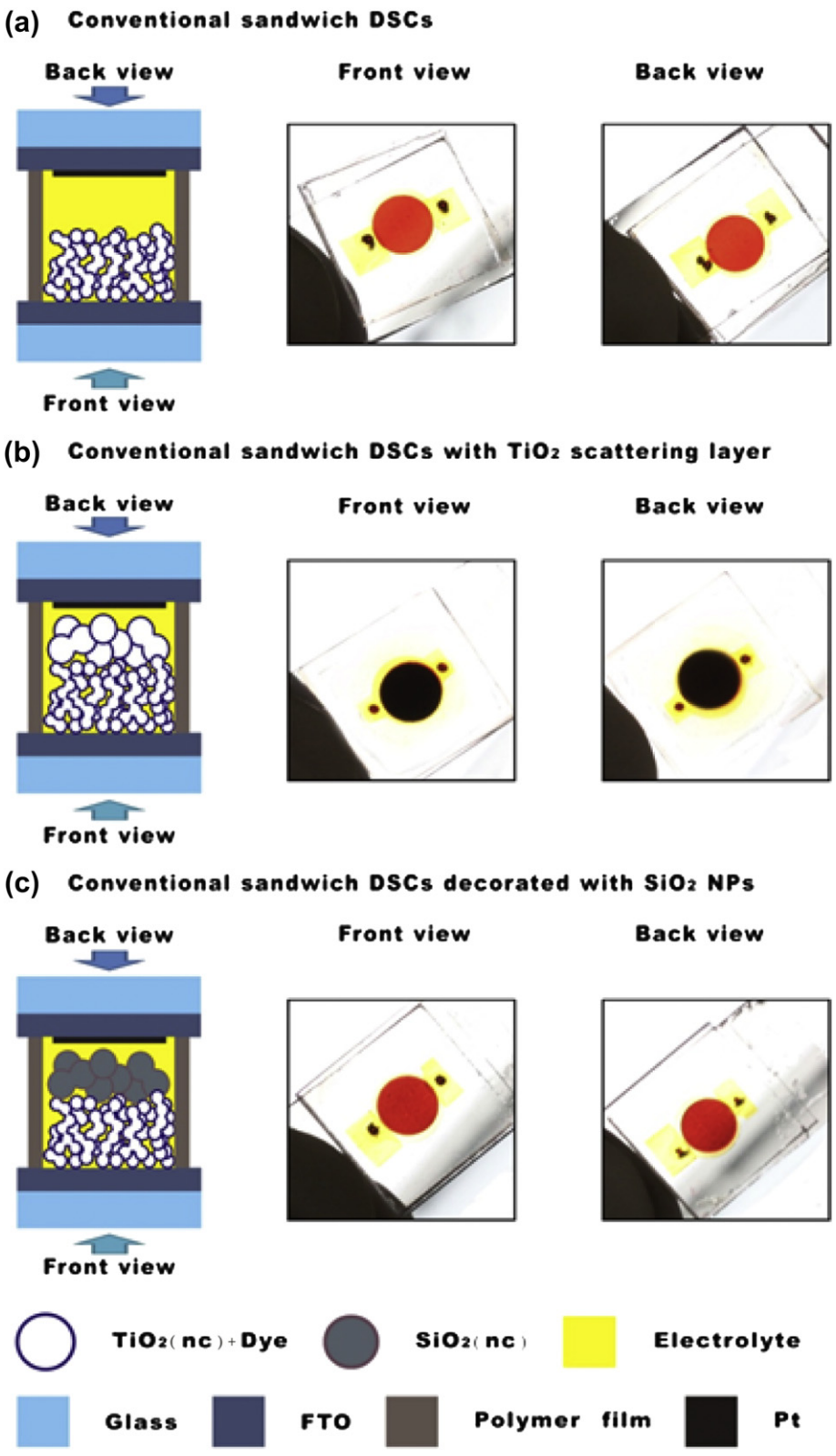

Fig. 1. Cell structures and photographies of DSCs (a) without and (b) with TiO_2 scattering layer, (c) DSCs decorated with SiO_2 NPs layer on TiO_2 porous electrode.

recent times, extensive research has been focused on novel bifacial and flexible solar cells for facilitating them in to advanced applications. Bifacial solar cell could produce up to 50% more electric power by collecting *albedo* radiation from the surroundings [3]. The lightweight and flexible metal foil, such as Ti foil and stainless steel, enable roll-to-roll mass production and make it possible to extend DSCs to newer applications. At this stage, it is very important to note that the conversion efficiency of the DSCs may also be improved

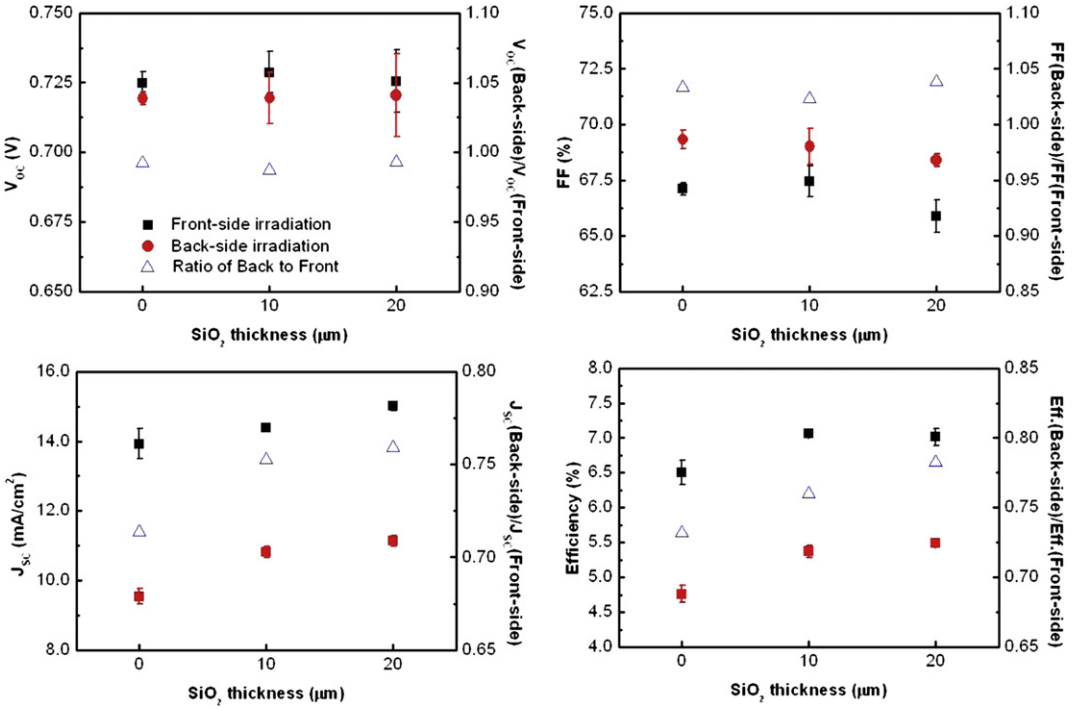

Fig. 2. Relationship between the photovoltaic characteristics of DSCs with SiO_2-decorated TiO_2 electrode (10 μm) containing different thicknesses of the SiO_2 particles. Black squares and red circles represent front- and back-side illumination, respectively. (For interpretation of the references to color in this figure legend, the reader is referred to the web version of this article.)

from back-side irradiation. Therefore, many attempts have been made to explore the high transparent counter electrodes [4–7], and the colorless electrolytes for DSC [8–14]. However, the incorporation of robust electrolytes for durable DSCs is still based on I^-/I_3^- system and reduction in the light absorption by this bulk electrolyte becomes a critical issue. In the present study, the influence of decoration of SiO_2 layer on TiO_2 electrode of the DSC on the light scattering and passage of incident light leading to effective performance during back- and front side irradiation is reported. The photoelectrochemical characteristics of DSCs have been extensively studied using UV–visible spectroscopy, electrochemical impedance spectroscopy (EIS) and incident photon conversion efficiency (IPCE). The influences of different concentrations of I_2 on the performance of Ti foil based sub-module DSC have also been examined.

2. Experimental

2.1. Preparation of TiO_2 electrode and device fabrication

Anatase TiO_2 nanoparticles (ca. 20 nm diameter) were hydrothermally prepared in a Ti-based autoclave as reported previously [15]. The screen-printable TiO_2 paste prepared by thorough mixing of 4.3 g of TiO_2 nanoparticle, 56 ml of ethyl cellulose, and 45 ml of terpineol was coated on 2.2 mm thick fluorine-doped tin oxide glass (FTO glass, Pilkington, TEC-8, 8 Ω square^{-1}) and 50 μm thick Ti foil, which was pre-treated with H_2O_2 for 8 h, by a screen-printing procedure. The screen-printed TiO_2 electrodes were annealed at 500 °C for 1 h in a stream of air. For comparison, we coated SiO_2 particles of different thicknesses on TiO_2 electrode. The SiO_2 paste was prepared by thorough mixing of 15 nm and 500 nm diameter SiO_2 ($w/w = 1/4$) with 56 ml of ethyl cellulose, and 45 ml of terpineol. The SiO_2 paste was coated on the top of TiO_2 film and similar annealing procedure as described above was followed. After cooling to room temperature, the TiO_2 electrodes were immersed in a N719 dye bath at 40 °C for 12 h. The dye solutions were prepared by adding 0.3 mM of N719 in a mixture of *tert*-butyl alcohol (*t*-BuOH) and AN ($v/v = 1/1$). The dyed anode was rinsed with AN, and then dried at 60 °C for 5 min. Thermally platinized FTO glass was used as the counter electrode and a low-volatility electrolyte with the composition of 0.8 M PMII, 0.05 M I_2, and 0.5 M NMBI in AN/MPN ($v/v = 1/1$) was employed. The active area of TiO_2 working electrode of small cell and sub-module are 0.28 cm^2 and 22.4 cm^2, respectively.

2.2. Photoelectrochemical and electrochemical impedance spectroscopy (EIS) measurements

Photoelectrochemical measurements were carried out at open circuit conditions after a period of continual light irradiation, being allowed to cool and equilibrate at room temperature. Solar

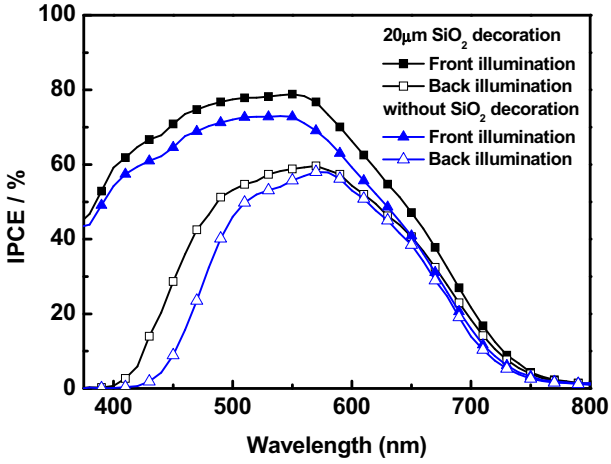

Fig. 3. Incident photo-to-conversion efficiency (IPCE) spectra of DSCs with and without 20 μm SiO_2 layer on TiO_2 electrodes for front-side and back-side irradiation.

Table 1
Photovoltaic characteristics and EIS elements of DSCs with and without SiO_2 layer (20 μm) on porous TiO_2 film (10 μm), at one sun irradiation (AM 1.5), and front- and back-illumination, respectively.

Electrode	J_{SC} (mA cm^{-2})	V_{OC} (V)	FF	η (%)	R_{ct1} (Ω)	R_{ct2} (Ω)	R_{ele} (Ω)
TiO_2 (front)	13.39	0.725	0.675	6.55	4.8	16.3	7.2
TiO_2 (back)	9.61	0.720	0.692	4.79	4.7	23.5	6.8
TiO_2/SiO_2 (back)	11.67	0.725	0.685	5.80	4.8	19.5	8.8

R_{ct1}: interface resistance between Pt electrode and electrolyte; R_{ct2}: interface resistance between TiO_2 and electrolyte; R_{ele}: diffusion resistance of electrolyte.

simulator (an AM 1.5, Yamashita Denso, YSS-100A) was used as the irradiation source for the current density–voltage (J–V). The intensity of simulated sunlight was calibrated to 100 mW cm^{-2} by using a silicon reference cell. Related data were collected by an electrochemical analyzer (Autolab, PGSTAT30) at 25 °C. For EIS measurements, we applied a forward bias set at the open circuit voltage (V_{OC}) with AC amplitude of 10 mV, between the working and counter electrodes, and the frequency range was fixed from 100 kHz to 100 mHz. The equivalent circuit model used for EIS analysis is similar with the previous reports [16,17].

3. Results and discussion

Schematic cell diagrams and photographies of rigid DSC without (a) and with TiO_2 (b) scattering layer, and DSCs decorated with SiO_2 mesoporous layer on TiO_2 porous electrode (c) are shown in Fig. 1. The solar cells become semi-transparent when no scattering layer is present on TiO_2 electrode. The semi-transparent nature still remains even for the photoanode coated with SiO_2 layer (Fig. 1(a) and (b)). However, by incorporating the TiO_2 scattering layer, the cell becomes darkened, which may be associated with excellent trapping of incident light by the TiO_2 particles (Fig. 1(c)). The above phenomenon is an evidence for the good performance of the solar cell containing TiO_2 scattering layer in the front-side irradiation. However, for back-side irradiation, TiO_2 scattering layer should not be used and the light absorption by the electrolyte takes place in the region of 400–600 nm. Therefore, decoration of SiO_2 mesoporous film on TiO_2 electrode was carried out for facilitating the passage of incident light, which in-turn reduces the light absorption by I^-/I_3^- in the electrolyte. The performance characteristics of DSC containing different thicknesses of SiO_2 nano-particles on TiO_2 electrode are shown in Fig. 2. There is no change in V_{OC} values, but J_{SC} increases and fill factor (FF) decreases with an increase in the thickness of the SiO_2 layer. For back-side irradiation, the increase in the J_{SC} is due to the presence of SiO_2 layer which contributes for the excellent light transmission. More the number of SiO_2 nano-particles present in bulk electrolyte, higher will be the incident light passing through the dyed-TiO_2 electrode, which can reduce the light absorption (350–600 nm), leading to an increase of J_{SC} by approximately 17.6%. For front side irradiation, the increase of J_{SC} is about 6.8% on account of the present of SiO_2 scattering layer, which is confirmed by recent literature studies [18,19]. A small decrease of FF (ca. 1%) is due to the increase of series resistance of DSC with SiO_2 layer. Fig. 3 shows the IPCE spectra of DSC with and without SiO_2 layer from back- and front-side irradiation. DSCs with SiO_2 layer exhibit high value of IPCE in the wavelength of 400–800 nm and 400–600 nm for front and back-side irradiation, respectively. The above study reveals that for both side illuminations, efficient light scattering is responsible for the red shift in the action spectra. DSC containing TiO_2 electrode decorated with SiO_2 layer exhibits a better performance when compared to their counterpart without SiO_2 layer and as a result of this, the efficiency increases from 6.55 to 7.10% (an increase of ca. 7.7% value) and 4.79–5.80% (an increase of ca. 17.4% value) for front and back-side irradiation, respectively (Table 1).

In addition, EIS was used for studying the performance of the bifacial DSCs (Fig. 4(a)). Generally, all the spectra of the DSCs exhibit three semicircles, which are assigned to electrochemical reaction at the Pt counter electrode (R_{ct1}), charge transfer at the dyed-TiO_2 electrode (R_{ct2}) and Warburg diffusion process of I^-/I_3^- in electrolyte (R_{ele}). The R_S and CPE represent series resistance and constant phase element (equivalent electrical circuit component that models the behavior of a double layer, an imperfect capacitor), respectively. Each semicircle was analyzed using a simple equivalent circuit model (Fig. 4(b)) and the characteristic parameters are listed in Table 1. It is noted that the R_s and R_{ct1} take a constant value of 25 and 4.8 Ω for front- and back irradiation respectively. The semicircle of R_{ct2} for back-side irradiation (23.5 Ω) is found to be higher than that of front-side irradiation (16.3 Ω), indicating a lengthy electron transport in the front side TiO_2 electrode. It is also observed that the value R_{ele} for front side irradiation is slightly higher than that of back-side irradiation.

The above phenomenon may be correlated with the fact that for front-side irradiation, the excited electrons are very close to the FTO substrate, and as a result of this, the transport of electron through I_3^- diffusion may take long time from the reduced dye to the Pt counter electrode in the narrow TiO_2 pore. On the other hand, in the case of back-side irradiation, the distance for electrons transportation is short as the excited dye is close to the Pt counter electrode. As a result of this, the ionic diffusion resistance of the electrolyte (R_{ele}) is low for back-side irradiation. These behaviors are also confirmed by recent literature [20].

Moreover, for back-side irradiation, DSC with SiO_2 layer obviously shows a drastic change in the cell performance, specifically an increase in the J_{SC} value from 9.61 to 11.67 mA cm^{-2}, as shown in Fig. 3 and Table 1. As noted in the EIS analysis (Fig. 4), a slight increase in the value of R_{ele} by the addition of porous SiO_2 layer may cause reduced movement of I^-/I_3^- in the bulk electrolyte. The decrease in the R_{ct2} value from 23.5 to 19.5 Ω may be due to the

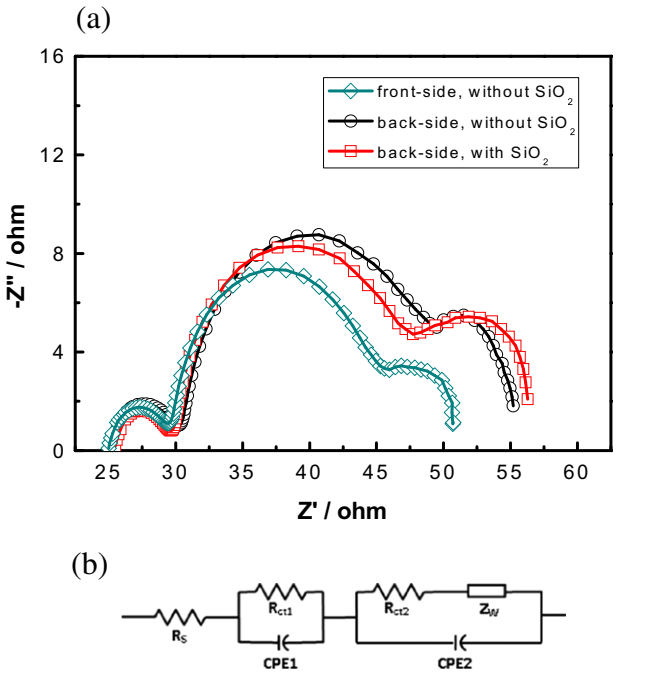

Fig. 4. (a) Nyquist plot of EIS analysis for DSCs with and without SiO_2 layer (20 μm) on porous TiO_2 electrode, from front-side and back-side irradiation at open-circuit voltage conditions. (b) The equivalent circuit plot of DSC in this study.

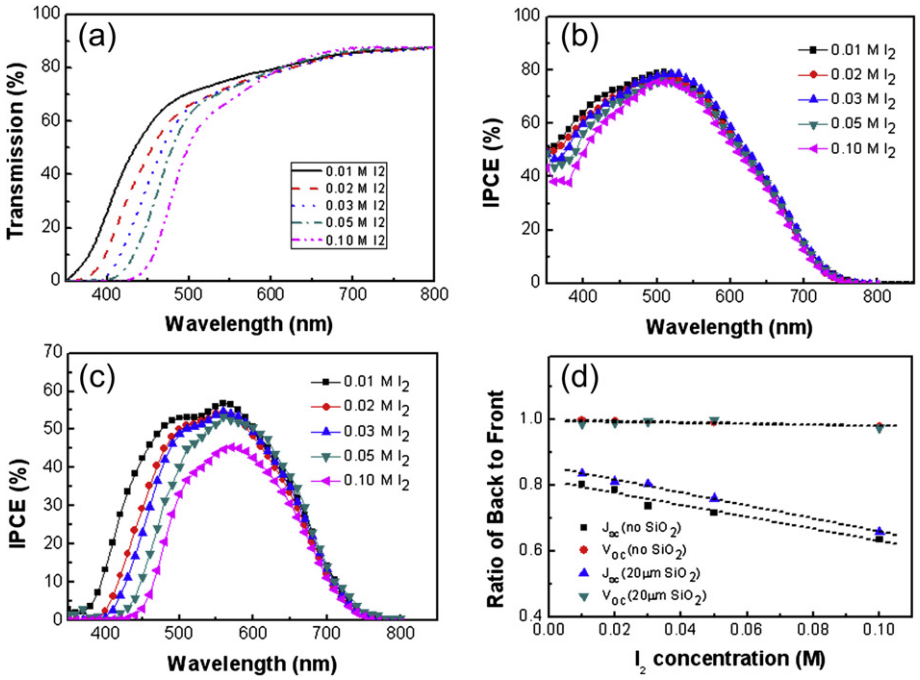

Fig. 5. (a) The UV–visible spectra of electrolytes containing various concentrations of I_2. (b) And (c) show the IPCE of DSCs for front- and and back-side irradiation respectively. (d) The relationship between J_{SC} and V_{OC} of DSCs with various I_2 concentrations in electrolytes.

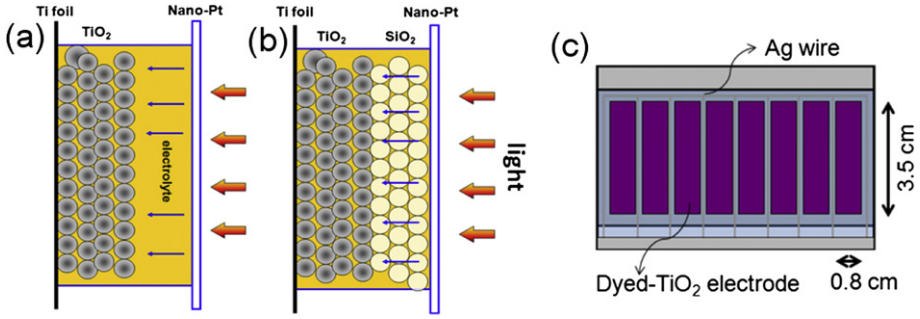

Fig. 6. Schematic diagrams of Ti foil based DSC without (a) and with SiO_2 layer (b) on TiO_2 porous electrode, (c) Ti foil based sub-module DSC (5 cm × 10 cm).

absorption of more incident light on the dyed-TiO_2 electrode through SiO_2 layer, which can generate high electron flux in the TiO_2 anode.

It is well known that I_2 exists in the electrolyte with iodides in the form of polyiodides such as I_3^- or I_5^-. An efficient transport of iodide and triiodide in the electrolyte is necessary for the good performance of a DSC, because the oxidized dye should be regenerated by I^- efficiently after the electrons from the excited state of the dye are injected into the conduction band of TiO_2 under illumination. At the same time, the electrons accumulated at the counter electrode through the external circuit will lead to concentration overpotential in the electrolyte and results in the loss of energy for the DSC, provided the electrons are transferred efficiently from the counter electrode to I_3^-. However, an increase in the content of I_2 (or I_3^-) leads to enhanced light absorption by the electrolyte in the visible range (Fig. 5(a)). In addition, excessive I_2 would also increase the dark reduction current. Therefore, a photoelectrochemical study on finding optimal ratio of I^-/I_3^- is necessary to achieve good performance for a DSC, especially for back-illuminated solar cell. The IPCE curves of DSCs for front-side and back-side illumination with different concentrations of I_2 in the electrolyte are shown in Fig. 5(b) and (c), respectively. DSC with front-side illumination exhibits decrease of visible light wavelength from 400 to 500 nm, but back-side illuminated DSC shows an obvious decrease of wavelength from 400 to 600 nm due to the absorption of part of incident light by I^-/I_3^- solution. The above results show that SiO_2 layer may be kept between electrodes in the back-side illuminated DSC path for good light transport. In Fig. 5(d), the ratio of J_{SC} corresponding to back- to front-side illumination increases from 0.67 to 0.83 and from 0.65 to 0.79 for the DSCs with and without SiO_2 layer, respectively, when the I_2 concentration decreases from 0.1 M to 0.01 M. The ratio of J_{SC} for back- to front-side is always high for DSC with SiO_2 layer and this indicates that

Table 2
Photovoltaic characteristics of Ti foil based DSCs with 20 μm SiO_2 layer on TiO_2 electrode containing various concentrations of I_2.

I_2 conc.	J_{SC} (mA cm^{-2})	V_{OC} (V)	FF	η (%)
0.05 M	11.83	0.711	0.739	6.21
0.04 M	12.20	0.732	0.727	6.49
0.03 M	12.72	0.734	0.724	6.76
0.03 M (without SiO_2)	11.25	0.740	0.725	6.04
0.02 M	12.92	0.745	0.690	6.64
0.01 M	12.90	0.750	0.665	6.43

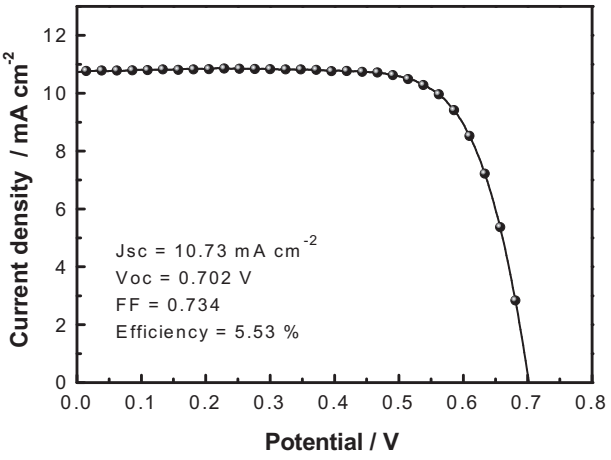

Fig. 7. The i–v curve of Ti foil based DSC sub-module (5 cm × 10 cm) with SiO_2 layer (20 μm) on TiO_2 electrode (15 μm) under illumination of 100 mW cm^{-2} (AM 1.5).

decorating SiO_2 layer on TiO_2 electrode is effective in increasing the intensity of incident light on the anode, especially for back-side illuminated DSC.

Furthermore, we also put this design as schematic in Fig. 6(a) and (b) for back-side illuminated DSC with and without SiO_2 respectively as well as in Fig. 6(c) for Ti foil based sub module DSC. The photoelectrochemical characteristic parameters of Ti foil based DSC with SiO_2 layer on TiO_2 electrode with different iodide concentrations are shown in Table 2. With a decrease in the iodide concentration, an initial hike in the J_{SC} value is noted, which may be due to the increase in incident photon and decrease in electron recombination rate. However, the decrease of FF values from 0.74 to 0.67 is due to the decrease in ionic conductivity of electrolyte. The best J_{SC} and FF values of 12.72 mA cm^{-2} and 0.72 respectively are obtained for the DSC containing an optimal concentration of 0.03 M of I_2. This good performance may be associated with the higher conductivity of Ti foil than FTO glass. Finally, as shown in Fig. 6(c), we scale up the solar cell area from 0.28 cm^2 to 5 cm × 10 cm of sub-module DSC with Ag wire pattern, and the corresponding i–v curves are shown in Fig. 7. With the optimization of Ag wire pattern (i.e. wide and aspect ratio of Ag wire) and TiO_2 electrode coating process, a good performance of Ti foil based sub-module DSC with J_{SC} of 10.73 mA cm^{-2}, V_{OC} of 0.702 V, FF of 0.734 and cell conversion efficiency of 5.54% was obtained under 100 mW cm^{-2} (AM 1.5).

4. Conclusions

In this study, the excellent performance of bifacial and back-illuminated dye-sensitized solar cells by the decoration of SiO_2 mesoporous layer with TiO_2 was successfully demonstrated. The photocurrent of front- and back-illuminated DSC with the optimal thickness of SiO_2 (20 μm) enhances owing to high scattering and broad optical channel in the electrolyte The enhancement in cell conversion efficiency of the DSCs from 6.55 to 7.10% and 4.79–5.80% are noted for front and back-side irradiation, respectively. The ratios of the respective efficiencies for front and back-side irradiation also increase from 0.72 to 0.82. Finally, by incorporating this modification on Ti foil based flexible DSC with optimum concentration of I_2, a good conversion efficiencies of 6.76 and 5.54% for 0.28 cm^2 small cell and 5 cm × 10 cm sub-module DSC, respectively, were obtained under 100 mW cm^{-2} (AM 1.5).

Acknowledgment

The authors acknowledge the financial support from the National Science Council (NSC) of Taiwan through project No. NSC-101-2731-M-008-003-MY3 and 101-2811-M-008-072-. C.G. Wu and K.M. Lee specially thank the NSC of Taiwan to fund the AROPV Lab through project No. NSC-99-2119-M-008-022-MY2.

References

[1] C.Y. Chen, M. Wang, J.Y. Li, N. Pootrakulchote, L. Alibabaei, C. Ngoc-le, J.D. Decoppet, J.H. Tsai, C. Grätzel, C.G. Wu, S.M. Zakeeruddin, M. Grätzel, ACS Nano 3 (2009) 3103–3109.
[2] A. Yella, H.W. Lee, H.N. Tsao, C. Yi, A.K. Chandiran, Md. K. Nazeeruddin, Eric W.G. Diau, C.Y. Yeh, S.M. Zakeeruddin, M. Grätzel, Science 334 (2011) 629–634.
[3] A. Hübner, A.G. Aberle, R. Hezel, Appl. Phys. Lett. 70 (1997) 1008–1010.
[4] W.J. Hong, Y.X. Xu, G.W. Lu, C. Li, G.Q. Shi, Electrochem. Commun. 10 (2008) 1555–1558.
[5] M.K. Wang, A.M. Anghel, B. Marsan, N.L.C. Ha, N. Pootrakulchote, S.M. Zakeeruddin, M. Grätzel, J. Am. Chem. Soc. 131 (2009) 15976–15977.
[6] L.L. Chen, W.W. Tan, J.B. Zhang, X.W. Zhou, X.L. Zhang, Y. Lin, Electrochim. Acta 55 (2010) 3721–3726.
[7] Y.L. Lee, C.L. Chen, L.W. Chong, C.H. Chen, Y.F. Liu, C.F. Chi, Electrochem. Commun. 12 (2010) 1662–1665.
[8] M. Cheng, X. Yang, S. Li, X. Wang, L. Sun, Energy Environ. Sci. 5 (2012) 6290–6293.
[9] A.M. Spokoyny, T.C. Li, O.K. Farha, C.W. Machan, C. She, C.L. Stern, T.J. Marks, C.A. Mirkin, Angew. Chem. Int. Ed. 49 (2010) 5339–5343.
[10] T. Daeneke, T.H. Kwon, A.B. Holmes, N.W. Duffy, U. Bach, L. Spiccia, Nat. Chem. 3 (2011) 213–217.
[11] D. Zhou, Q. Yu, N. Cai, P. Wang, Energy Environ. Sci. 4 (2011) 2030–2034.
[12] F.M. Sandra, E.A. Gibson, E. Gabrielsson, L. Sun, G. Boschloo, A. Hagfeldt, J. Am. Chem. Soc. 132 (2010) 16714–16724.
[13] J. Xia, N. Masaki, M. Lira–Cantu, Y. Kim, K. Jiang, S. Yanagida, J. Am. Chem. Soc. 130 (2008) 1258–1263.
[14] Z.S. Wang, K. Sayama, H. Sugihara, J. Phys. Chem. B 109 (2005) 22449–22455.
[15] S. Ito, T.N. Murakami, P. Comte, P. Liska, C. Gräzel, M.K. Nazeeruddin, M. Grätzel, Thin Solid Films 516 (2008) 4613–4619.
[16] M. Adachi, M. Sakamoto, J. Jiu, Y. Ogata, S. Isoda, J. Phys. Chem. B 110 (2006) 13872–13880.
[17] H.M. Cheng, W.H. Chiu, C.H. Lee, S.Y. Tsai, W.F. Hsieh, J. Phys. Chem. C 112 (2008) 16359–16364.
[18] T. Yasuda, S. Ikeda, S. Furukawa, Dyes Pigm. 86 (2010) 278–281.
[19] K.M. Lee, V. Suryanarayanan, K.C. Ho, Solar Energy Mater. Solar Cells 90 (2006) 2398–2404.
[20] P.T. Hsiao, Y.J. Liou, H. Teng, J. Phys. Chem. C 115 (2011) 15018–15024.